Available online at www.sciencedirect.com
SCIENCE DIRECT®
Marine Geology 199 (2003) 205–220
MARINE GEOLOGY
INTERNATIONAL JOURNAL OF MARINE GEOLOGY, GEOCHEMISTRY AND GEOPHYSICS
www.elsevier.com/locate/margeo

Sr/Ba in barite: a proxy of barite preservation in marine sediments?

P. van Beek *, J.-L. Reyss, P. Bonte, S. Schmidt

Laboratoire des Sciences du Climat et de l'Environnement, Domaine du CNRS, 91198 Gif-sur-Yvette, France

Received 30 July 2002; accepted 23 June 2003

Abstract

The observation by Bertram and Cowen [J. Mar. Res. 55 (1997) 577–593] that the strontium content of marine barite decreased from the water column to the deep-sea floor suggested that the Sr/Ba ratio in barite was sensitive to barite dissolution. Following this observation, we have investigated the potential of using the Sr/Ba ratio in barite as a proxy of barite preservation by separating barite crystals from sediment cores collected at different water depths in the equatorial Pacific and in the Southern Ocean. Our investigations do not reveal significant downcore variations in the Sr/Ba ratios during the Holocene period in the two basins and up to a few hundred thousand years in the equatorial Pacific. However, a comparison of the mean Sr/Ba ratios in individual cores suggests that the Sr/Ba ratios in barite decrease with increasing water depth, a feature that could be related to dissolution of barite crystals during settling to the deep-sea floor and/or at the sediment–water interface. If confirmed, the Sr/Ba ratios in barite could be used to infer the intensity of barite dissolution and the state of preservation of barite crystals in sediments. Such information could be employed usefully in paleoproductivity reconstructions for the purpose of distinguishing between productivity and dissolution signals affecting barite distributions in marine sediments.

Keywords: barite; strontium; dissolution; equatorial Pacific; Southern Ocean

1. Introduction

Over the last decades, many studies have focused on the search for reliable geochemical tracers to reconstruct past oceanic conditions and productivity changes that could bring insight into the role played by the oceans in the glacial/interglacial variations of atmospheric CO_2 concentrations as recorded in ice cores (Barnola et al., 1987; Neftel et al., 1988). From this point of view, marine barite ($BaSO_4$) appears to be a promising tracer that covers a wide range of applications. Barite crystals constitute a universal component of suspended matter that carries most of the particulate barium in the water column (Dehairs et al., 1980; Bishop, 1988). Higher barite fluxes characterize intermediate waters and deep-sea sediments underlying areas of high productivity (Schmitz, 1987; Dehairs et al., 1992;

* Corresponding author. Present address: LEGOS (CNRS/CNES/IRD/UPS), Observatoire Midi-Pyrénées 14, avenue Edouard Belin, 31400 Toulouse, France. Tel.: +33-561332933; Fax: +33-561253205.
E-mail addresses: pvanbeek@lsce.cnrs-gif.fr (P. van Beek), reyss@lsce.cnrs-gif.fr (J.-L. Reyss).

0025-3227/03/$ – see front matter © 2003 Elsevier B.V. All rights reserved.
doi:10.1016/S0025-3227(03)00220-2

Gingele and Dahmke, 1994; Paytan et al., 1996a). From this observation, relationships between barite fluxes derived from sediment trap data, export of organic matter and the associated productivity in surface oceans have been proposed (Dymond et al., 1992; François et al., 1995), thus allowing barite accumulated in sediments to be used as a proxy for paleoproductivity reconstructions (Schmitz, 1987; Gingele and Dahmke, 1994; Paytan et al., 1996a; Nürnberg et al., 1997). In addition, because of its formation in the water column, barite provides the opportunity to record seawater elemental composition, like Sr (Paytan et al., 1993; Martin et al., 1995; Bertram and Cowen, 1997), rare earths (Guichard et al., 1979; Martin et al., 1995) and S (Paytan et al., 1998). Being chemical analogues of barium, radium isotopes (in particular, ^{226}Ra, $T_{1/2}=1602$ a and ^{228}Ra, $T_{1/2}=5.75$ a) are also incorporated in barite crystals. ^{226}Ra/Ba (Moore and Dymond, 1991) and ^{228}Ra/^{226}Ra (Legeleux and Reyss, 1996) ratios measured in particulate matter collected with sediment traps have therefore been used to trace both the formation and settling of barite in the water column. Finally, the decay of ^{226}Ra activities in barite that accumulates in deep-sea sediments provides a means to date Holocene sediments (Paytan et al., 1996b; van Beek and Reyss, 2001; van Beek et al., 2002).

Paradoxically, although sedimentary barite has been widely used for paleoceanographic investigations, many unknowns remain. The mechanism of barite formation is still poorly known. Because the water column is mostly undersaturated with respect to barite (Church and Wolgemuth, 1972), barite crystals are assumed to form within microenvironments of settling flocs in the upper water column (Dehairs et al., 1980; Moore and Dymond, 1991; Legeleux and Reyss, 1996). It has been proposed that barite supersaturation within microenvironments was achieved by Ba and S release from decomposing organic matter exported from the euphotic layer (Chow and Goldberg, 1960; Dehairs et al., 1980, 1990; Bishop, 1988, 1991; Stroobants et al., 1991). The dissolution of acantharian-derived celestite may also constitute a significant source of Ba and S for barite formation (Bernstein et al., 1992, 1998). In addition, the fate of barite crystals (preservation versus dissolution), either within the water column or during early diagenesis is poorly characterized leading to uncertainties in interpreting sedimentary barite records.

The oceanic distribution of dissolved Ba indicates biological uptake in the upper water column and regeneration at depth (Wolgemuth and Broecker, 1970). Because sediment porewaters are generally at saturation with respect to barite under oxic and suboxic conditions, barite seems to be well preserved relative to most of the other biogenic phases. Estimates indicate that ca. 30% of the barite fluxes to the ocean floor is buried in the sediment (Dymond et al., 1992; Paytan and Kastner, 1996). Studies carried out using benthic chambers nevertheless point to a geographic heterogeneity in barite burial efficiencies (McManus et al., 1999). Dymond et al. (1992) suggested that barite burial efficiency was likely to vary in relationship with the mass accumulation rate: in sediments displaying a high accumulation rate barite would have a shorter period of time to efficiently communicate with undersaturated bottom waters, thus enhancing barite preservation. Following this argument, a higher barite preservation is expected in continental margin environments, a trend that is not always found as shown by Kumar et al. (1996). Moreover, it has been recently proposed through thermodynamic calculations that equilibrium between barite and seawater may be reached in several places of the world's oceans (Monnin et al., 1999; Rushdi et al., 2000). These findings have led these authors to define barite saturation horizons in the different regions investigated. The resulting implication is that barite preservation in marine sediments may thus depend on both the geographic location and the depth of the sediments in the water column. A better understanding of the geochemical behavior of barite, especially during early diagenesis, is therefore required before barite can be used with confidence in paleoceanographic studies.

Strontium, chemical analogue of barium, is incorporated in barite during its formation in the water column. Strontium concentration in barite reaches a few percent (Dehairs et al., 1980; Bishop, 1988). Bertram and Cowen (1997) reported a

lower Sr content in barite crystals from superficial sediments relative to those from the water column, which they attributed to barite dissolution in undersaturated waters. Here we report Sr/Ba ratios of barite separated from several cores collected between 2000 and 5000 m in the equatorial Pacific and in the Southern Ocean to assess the heterogeneity of the Sr/Ba ratio in these two regions and with changing water depth. Ratios are reported for the Holocene period for all cores and up to about 600 000 years for two locations in the equatorial Pacific. These investigations are designed to provide information on the geochemical behavior (preservation versus dissolution) of barite crystals during early diagenesis and to test the potential of the Sr/Ba ratio in barite of being an indicator of the preservation state of barite crystals.

2. Materials and methods

2.1. Ba and Sr contents in barite

Barite crystals were chemically separated from equatorial Pacific cores (Fig. 1 and Table 1) using the protocol proposed by Paytan et al. (1993), slightly modified (van Beek and Reyss, 2001). This protocol consists of sequential leaching steps that remove the different Ba-rich phases – other than barite – of the sediment (i.e. calcium carbonate, oxides and hydroxides, organic matter, opal and alumino-silicates). For cores from the Southern Ocean (Fig. 1 and Table 1), a heavy liquid separation was applied, employing 'LST Fast-float' (i.e. a solution of sodium heteropolytungstates in water at 2.8 g cm^{-3}) as performed by van Beek et al. (2002). Sodium polytungstate (SPT) with a similar density was applied to several samples from multicore PS1768-1. The dense fractions recovered with the latter technique contain barite crystals that have been separated from biogenic silica because of the difference in density between barite crystals and opal (4.5 g cm^{-3} and 2.2 g cm^{-3}, respectively).

Quantification of Ba and Sr contents in the separated samples was performed by instrumental neutron activation analysis (INAA). Standards and approximately 20 barite samples at a time were introduced into the Osiris reactor of Saclay (Laboratoire Pierre Süe) for an irradiation of 6 min at a flux of 0.9×10^{14} neutrons cm^{-2} s^{-1}. Standards and samples were then measured for their gamma activity using the germanium detectors placed at the Laboratoire des Sciences du Climat et de l'Environnement, Gif-sur-Yvette, France. ^{131}Ba ($T_{1/2}=12$ days) and ^{85}Sr ($T_{1/2}=64$ days) activities were measured at 496.3 and 514.0 keV, respectively, three weeks after irradiation to allow the decay of short half-life radioisotopes within the samples. Errors associated with the method include (1) error in the weight of the samples, (2) error related to the gamma counting (counting statistics; counting geometries that may be slightly different in between the samples; position of the sample on the detector during counting that may also slightly vary from one sample to another), and (3) error that results from the comparison in between different batches of samples (as INAA is on 20 samples at a time).

A $BaCO_3$ standard was employed to quantify the Ba content in the samples. In order to use a single standard for determining both Ba and Sr contents in the samples, the Sr content in the $BaCO_3$ standard was quantified using SGR1 standard (Green River shale). $BaCO_3$ and SGR1 standards were put together in 10 different batches of samples (reproducibility experiment). A Sr concentration of $20\,530\pm1910$ ppm (10 independent measurements) was thus obtained for the $BaCO_3$ standard. The Sr/Ba mole ratio in the $BaCO_3$ standard can therefore be estimated at 0.0462 ± 0.0047 (considering a 4% error associated with the estimate of the Ba concentration as deduced from reproducibility experiments). The use of a single standard with a known Sr/Ba ratio allows the error on the estimate of the Sr/Ba ratio in the barite samples to be minimized. The resulting precision of the Sr/Ba ratio measurements in the barite samples is estimated at 7%.

2.2. Temporal framework

^{14}C ages in cores ERDC112, PLDS72 and PLDS79 were published by Berger and Killingley (1982) and Berger et al. (1983). In core KTB03,

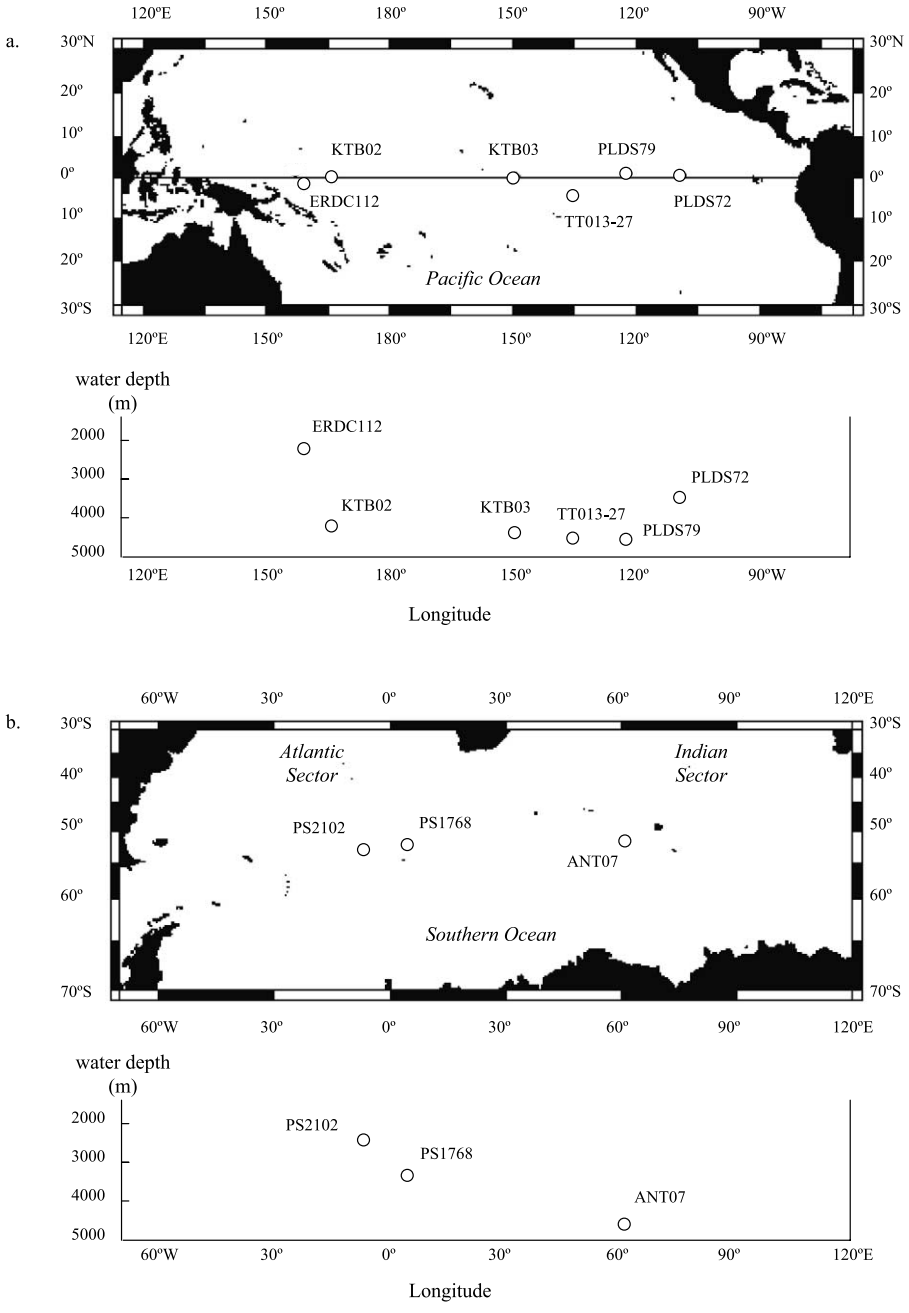

Fig. 1. Location and recovery depth of cores investigated in this study. (a) Equatorial Pacific. (b) Southern Ocean.

AMS ^{14}C ages were obtained using planktic foraminifers (*Pulleniatina obliquiloculata*) (van Beek et al., in press). Radiocarbon ages determined on the bulk carbonate fraction were available in core TT013-27 (DeMaster et al., 1996; van Beek et al., in press). Sedimentation rate estimates deduced from the ^{226}Ra decay in barite ($T_{1/2} = 1602$ a) for cores KTB03, TT013-27, KTB02, ERDC112,

Table 1
Core locations. Sedimentation rates estimated in the cores either from the $^{226}Ra_{ex}$ decay in barite or from cal. ^{14}C ages are also reported (see references)

Core	Location		Core type	Water depth (m)	Sedimentation rate (cm ka^{-1})		Ref.
					$^{226}Ra_{ex}$ in barite	Cal. ^{14}C	
PLDS72	1°01′N, 109°16′W	East equatorial Pacific	Box Core	3626	2.4	2.7	Berger and Killingley (1982), Berger et al. (1983), van Beek et al. (in press)
PLDS79	1°05′N, 122°15′W	East equatorial Pacific	Box Core	4542	3.3	2.4	Berger and Killingley (1982), van Beek et al. (in press)
KTB03	0°02′N, 150°15′W	Central equatorial Pacific	Multicore	4436	2.3/2.6	1.7/3.3	van Beek and Reyss (2001), van Beek et al. (in press)
KGL03	0°01′N, 149°56′W	Central equatorial Pacific	Gravity Core	4469	–	–	van Beek and Reyss (2001)
KGL04	0°00′S, 149°51′W	Central equatorial Pacific	Gravity Core	4466	–	–	van Beek and Reyss (2001)
TT013-27	2°53′S, 139°50′W	Central equatorial Pacific	Multicore	4550	2.0/2.6	1.8	DeMaster et al. (1996), van Beek et al. (in press)
ERDC112	1°38′S, 159°14′E	West equatorial Pacific	Box Core	2169	3.2	2.6	Berger and Killingley (1982), van Beek et al. (in press)
KTB02	0°14′N, 166°26′E	West equatorial Pacific	Multicore	4346	1.0	–	van Beek and Reyss (2001), van Beek et al. (in press)
KGL02	0°03′N, 166°45′E	West equatorial Pacific	Gravity Core	4376	–	–	van Beek and Reyss (2001)
PS2102-2	53°04′S, 4°59′W	Southern Ocean, Atlantic Sector	Gravity Core	2390	31.5	–	van Beek et al. (2002)
PS1768-1	52°35′S, 4°28′E	Southern Ocean, Atlantic Sector	Multicore	3298	–	–	Frank (1996)
PS1768-8	52°36′S, 4°29′E	Southern Ocean, Atlantic Sector	Gravity Core	3270	–	6.4	Frank (1996)
ANT07	51°58′S, 61°07′E	Southern Ocean, Indian Sector	Multicore	4724	9.2		This study

ERDC83, PLDS72 and PLDS79 can be found in van Beek et al. (in press). For cores PS2102-2 and PS1768-8 collected in the Southern Ocean, AMS ^{14}C measurements performed on planktic foraminifers were available (van Beek et al. (2002) and Frank (1996), respectively). An estimate of the sedimentation rate using the ^{226}Ra decay in barite in core PS2102-2 can also be found in van Beek et al. (2002). A summary of the sedimentation rates estimated for the cores investigated in this study either by the ^{14}C technique or by measuring the ^{226}Ra decay in barite is reported in Table 1.

As no temporal framework was available for core ANT07 from the Indian sector of the Southern Ocean, a sedimentation rate was estimated using the ^{226}Ra decay in barite, as performed in core PS2102-2 (van Beek et al., 2002). ^{226}Ra activities were measured in the dense separated fractions using low-background, well-type germanium detectors located in the underground laboratory of Modane in the French Alps (Reyss et al., 1995). The ^{226}Ra activities were corrected for the ^{226}Ra in equilibrium with ^{238}U, as measured by INAA (Table 2). The resulting excess ^{226}Ra activities ($^{226}Ra_{ex}$) were then normalized to the barite content to remove the variation in the barite content from one sample to another due to dilution by the dense material (i.e. heavy minerals) that remained like barite in the separated fractions. Below the upper 10-cm mixed layer, the exponential decay of the ^{226}Ra activities in barite with sediment depth allows us to estimate a sedimentation rate for this core (Fig. 2). This method indicates that core ANT07 provides a record for the last 3000 years. However, it must be stressed that the multicore section investigated is not long enough (1) to display a pronounced decay of ^{226}Ra activities in barite that would provide a more accurate sedimentation rate estimation and (2) to give any information on the ^{226}Ra activities that may be produced by unsupported ^{230}Th (see van Beek and Reyss, 2001). Because of the uncertainty on the correction for ^{226}Ra supported by ^{230}Th, the sedimentation rate estimation given for core ANT07 should be considered as an upper estimate.

For all cores, Sr/Ba investigations were conducted for the Holocene period, with some data reported for the end of the last deglaciation. KGL03 and KGL02 are gravity cores collected at the same location as KTB03 and KTB02, re-

Table 2
Results of the analysis performed in the dense fractions separated from core ANT07, Indian Sector of the Southern Ocean

Depth (cm)	^{226}Ra (dpm g^{-1}) dense fraction	$BaSO_4$ (%) (±5%) dense fraction	^{238}U (dpm g^{-1}) (±20%) dense fraction	$^{226}Ra_{ex}$ (dpm g^{-1}) dense fraction	$^{226}Ra_{ex}$ (dpm g^{-1}) Barite
0.5–1.5	557 ± 45	43.9	4.0	553 ± 45	1260 ± 121
1.5–3.0	864 ± 34	71.7	< 1.3	864 ± 34	1205 ± 77
4–5	838 ± 57	63.4	2.2	836 ± 57	1319 ± 112
5–6	980 ± 41	61.2	3.1	977 ± 41	1596 ± 105
7–8	967 ± 24	67.8	< 1.3	967 ± 24	1426 ± 80
9–10	901 ± 49	67.5	2.6	898 ± 49	1330 ± 99
10–11	854 ± 41	63.4	2.5	851 ± 41	1342 ± 94
11–12	714 ± 56	49.8	< 1.3	714 ± 56	1434 ± 134
12–13	820 ± 47	66.5	2.8	817 ± 47	1229 ± 94
13–14	888 ± 56	72.8	1.7	886 ± 56	1217 ± 99
14–15	656 ± 37	65.5	< 1.3	656 ± 36	1002 ± 75
15–16	571 ± 35	63.6	4.5	566 ± 35	890 ± 71
16–17	723 ± 16	63.4	1.3	722 ± 16	1139 ± 63
18–19	669 ± 28	59.5	< 1.3	669 ± 28	1124 ± 74
20–21	645 ± 15	66.1	1.9	643 ± 15	973 ± 54
21–22	614 ± 31	68.0	< 1.3	614 ± 31	903 ± 65
22–23	318 ± 29	48.6	3.2	315 ± 29	648 ± 68
23–24	496 ± 19	66.1	< 1.3	496 ± 19	750 ± 48
24–26.5	449 ± 17	68.5	2.4	447 ± 17	653 ± 41

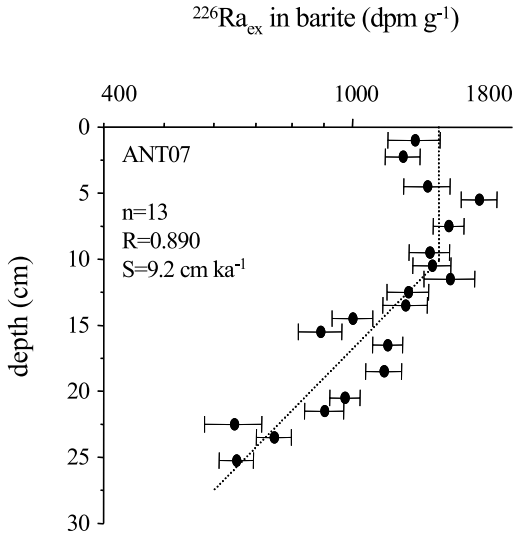

Fig. 2. Sedimentation rate estimate for core ANT07 as given by the exponential decay of ^{226}Ra activities in separated barite samples with increasing sediment depth. The ^{226}Ra activities measured in the separated samples were corrected for ^{238}U (providing excess ^{226}Ra, noted $^{226}Ra_{ex}$) and normalized to the barite content.

spectively. These cores therefore allow us to carry out Sr/Ba investigations on barite crystals from the equatorial Pacific up to about 600 000 years as deduced from $^{230}Th_{ex}$ sedimentation rates (van Beek and Reyss, 2001).

3. Results and discussion

3.1. Sr/Ba ratio in marine barite

Sr/Ba ratios measured in the separated barite samples are reported in Table 3. Samples separated from the sediment may contain impurities – mainly heavy minerals, such as TiO_2 minerals, monazite, zircon – that resist, like barite, the chemical treatment (Paytan et al., 1993; Martin et al., 1995; van Beek and Reyss, 2001). This is particularly true (1) for cores from the Southern Ocean because the heavy liquid technique employed does not allow the separation of barite from the other dense phases of the sediment, and (2) for core ERDC112 with a higher content of detrital material, which makes barite separation more complicated (Table 2; van Beek et al., in press). However, we expect the Ba and Sr contributions from these heavy minerals to be insignificant given that both are major constituents in barite crystals. Sr/Ba ratios can therefore be strictly related to barite crystals.

Sr/Ba ratios in barite separated from equatorial Pacific cores are displayed versus sediment depth in Fig. 3, while Fig. 4 puts together the Sr/Ba ratios obtained in the Southern Ocean cores. Sr/Ba ratios do not exhibit pronounced variations with sediment depth. Some cores display a higher scatter in the Sr/Ba ratios (i.e. core PS1768-8) but no trend seems to emerge, suggesting rather an analytical or a statistical scatter. Some other cores may exhibit downcore variability (see cores ERDC112, PLDS72, KTB03, TT013-27, PS2102-2). However, given the error bars on the ratios, it is difficult to define any clear trend. We therefore considered that no significant variation existed in the investigated cores. Mean Sr/Ba ratios were determined for each core and are reported in Figs. 3 and 4. The estimate of mean downcore Sr/Ba ratios allows us to partly remove the statistical and/or analytical fluctuations, thus providing a more accurate value for each core. Mean ratios range from 0.0350 to 0.0464 in barite samples from the equatorial Pacific and from 0.0364 to 0.0466 in barite samples from the Southern Ocean.

The study of the Sr/Ba ratios has been extended up to approximately 600 000 years in the central (KGL03/KGL04) and eastern (KGL02) equatorial Pacific. Mean Sr/Ba ratios found in cores KGL03/KGL04 appear to be identical to those found in barite samples from core KGL02. These results are also consistent with the ratios found during the Holocene period in cores KTB03 and KTB02 collected at the same location as cores KGL03/KGL04 and KGL02, respectively (Fig. 5).

Dehairs et al. (1980) and Bertram and Cowen (1997) reported large variations in the Sr/Ba ratio of barite collected in the water column (i.e. in between 0 and 26 mol% $SrSO_4$; Bertram and Cowen, 1997), in comparison with our estimates that range from 4 to 6 mol% $SrSO_4$. The smaller range in this study may result from the methodology, which integrates the ratios of several milli-

Table 3
Sr/Ba mole ratios measured in barite samples

Depth (cm)	Core	Separation method used	Sr/Ba (±7%)
3	PS2102-2	LST	0.0428
10	PS2102-2	LST	0.0482
20	PS2102-2	LST	0.0435
30	PS2102-2	LST	0.0492
36	PS2102-2	LST	0.0422
40	PS2102-2	LST	0.0517
50	PS2102-2	LST	0.0532
52	PS2102-2	LST	0.0468
60	PS2102-2	LST	0.0512
70	PS2102-2	LST	0.0451
80	PS2102-2	LST	0.0484
90	PS2102-2	LST	0.0466
92	PS2102-2	LST	0.0413
100	PS2102-2	LST	0.0431
110	PS2102-2	LST	0.0536
119	PS2102-2	LST	0.0478
129	PS2102-2	LST	0.0496
139	PS2102-2	LST	0.0537
149	PS2102-2	LST	0.0465
159	PS2102-2	LST	0.0441
169	PS2102-2	LST	0.0438
179	PS2102-2	LST	0.0453
189	PS2102-2	LST	0.0458
199	PS2102-2	LST	0.0461
205	PS2102-2	LST	0.0509
212	PS2102-2	LST	0.0532
225	PS2102-2	LST	0.0478
245	PS2102-2	LST	0.0467
255	PS2102-2	LST	0.0402
265	PS2102-2	LST	0.0462
275	PS2102-2	LST	0.0385
285	PS2102-2	LST	0.0392
295	PS2102-2	LST	0.0464
Mean	PS2102-2		0.0466 ± 0.0042
2–3	PS1768-1	LST	0.0524
5–7	PS1768-1	LST	0.0474
7–10	PS1768-1	LST	0.0431
7–10	PS1768-1	SPT	0.0428
10–13	PS1768-1	SPT	0.0384
16.5–20	PS1768-1	SPT	0.0449
20–24	PS1768-1	SPT	0.0402
24–28	PS1768-1	LST	0.0450
24–28	PS1768-1	SPT	0.0379
32	PS1768-8	LST	0.0487
35	PS1768-8	LST	0.0479
37	PS1768-8	LST	0.0502
40	PS1768-8	LST	0.0458
45	PS1768-8	LST	0.0468
50	PS1768-8	LST	0.0543
55	PS1768-8	LST	0.0453
65	PS1768-8	LST	0.0472
70	PS1768-8	LST	0.0523
85	PS1768-8	LST	0.0485
90	PS1768-8	LST	0.0383
91	PS1768-8	LST	0.0515
95	PS1768-8	LST	0.0456
101	PS1768-8	LST	0.0554
111	PS1768-8	LST	0.0544
116	PS1768-8	LST	0.0440
120	PS1768-8	LST	0.0448
140	PS1768-8	LST	0.0364
160	PS1768-8	LST	0.0461
170	PS1768-8	LST	0.0470
180	PS1768-8	LST	0.0465
Mean	PS1768		0.0463 ± 0.0050
0.5–1.5	ANT07	LST	0.0309
1.5–3.0	ANT07	LST	0.0374
4–5	ANT07	LST	0.0375
5–6	ANT07	LST	0.0370
7–8	ANT07	LST	0.0351
9–10	ANT07	LST	0.0353
10–11	ANT07	LST	0.0368
11–12	ANT07	LST	0.0347
12–13	ANT07	LST	0.0383
13–14	ANT07	LST	0.0372
14–15	ANT07	LST	0.0339
15–16	ANT07	LST	0.0363
16–17	ANT07	LST	0.0361
18–19	ANT07	LST	0.0357
20–21	ANT07	LST	0.0399
21–22	ANT07	LST	0.0354
22–23	ANT07	LST	0.0360
23–24	ANT07	LST	0.0353
24–26.5	ANT07	LST	0.0419
Mean	ANT07		0.0364 ± 0.0023
0–4	ERDC112	CT	0.0463
2–4	ERDC112	CT	0.0522
6–8	ERDC112	CT	0.0528
10–12	ERDC112	CT	0.0491
12–14	ERDC112	CT	0.0429
16–18	ERDC112	CT	0.0487
18–20	ERDC112	CT	0.0499
20–22	ERDC112	CT	0.0431
24–26	ERDC112	CT	0.0410
26–28	ERDC112	CT	0.0407
28–30	ERDC112	CT	0.0470
32–34	ERDC112	CT	0.0484
34–36	ERDC112	CT	0.0468
38–39	ERDC112	CT	0.0403
Mean	ERDC112		0.0464 ± 0.0042
2–3	PLDS72	CT	0.0413
4–5	PLDS72	CT	0.0393
7–8	PLDS72	CT	0.0409
11–12	PLDS72	CT	0.0374
18–19	PLDS72	CT	0.0445
21–22	PLDS72	CT	0.0432
24–25	PLDS72	CT	0.0363

Table 3 (*Continued*).

Depth (cm)	Core	Separation method used	Sr/Ba (±7%)
28–29	PLDS72	CT	0.0369
34–35	PLDS72	CT	0.0412
38–39	PLDS72	CT	0.0412
Mean	PLDS72		0.0402 ± 0.0028
0.5	KTB03V	CT	0.0401
1.5	KTB03V	CT	0.0366
3.5	KTB03V	CT	0.0364
4.5	KTB03V	CT	0.0355
6.5	KTB03V	CT	0.0373
7.5	KTB03V	CT	0.0424
9.5	KTB03V	CT	0.0406
10.5	KTB03V	CT	0.0377
12.5	KTB03V	CT	0.0432
14.5	KTB03V	CT	0.0420
16.5	KTB03V	CT	0.0378
18.5	KTB03V	CT	0.0409
19.5	KTB03V	CT	0.0378
20.5	KTB03V	CT	0.0429
22.5	KTB03V	CT	0.0394
24.5	KTB03V	CT	0.0357
26.5	KTB03V	CT	0.0421
30.5	KTB03V	CT	0.0347
31.5	KTB03V	CT	0.0336
32.5	KTB03V	CT	0.0359
Mean	KTB03V		0.0386 ± 0.0030
6	KGL03	CT	0.0375
14	KGL03	CT	0.0392
44	KGL03	CT	0.0367
46.5	KGL03	CT	0.0352
50.5	KGL03	CT	0.0356
57	KGL03	CT	0.0314
86	KGL03	CT	0.0361
156	KGL03	CT	0.0435
306	KGL03	CT	0.0360
367	KGL03	CT	0.0400
455	KGL04	CT	0.0380
456	KGL03	CT	0.0360
502	KGL03	CT	0.0424
546	KGL03	CT	0.0378
606	KGL03	CT	0.0419
605	KGL04	CT	0.0379
756	KGL03	CT	0.0375
918	KGL03	CT	0.0385
1066	KGL03	CT	0.0352
Mean	KGL03/04		0.0377 ± 0.0029
1.5	KTB02 I	CT	0.0337
2.5	KTB02 I	CT	0.0378
4.5	KTB02 I	CT	0.0352
6.5	KTB02 I	CT	0.0396
7.5	KTB02 I	CT	0.0354
9.5	KTB02 I	CT	0.0382
10.5	KTB02 I	CT	0.0391
11.5	KTB02 I	CT	0.0416
12.5	KTB02 I	CT	0.0352
14.5	KTB02 I	CT	0.0373
16.5	KTB02 I	CT	0.0400
18.5	KTB02 I	CT	0.0420
19.5	KTB02 I	CT	0.0369
20.5	KTB02 I	CT	0.0429
22.5	KTB02 I	CT	0.0375
24.5	KTB02 I	CT	0.0375
25.5	KTB02 I	CT	0.0339
27.5	KTB02 I	CT	0.0428
28.5	KTB02 I	CT	0.0364
30.5	KTB02 I	CT	0.0385
31.5	KTB02 I	CT	0.0438
Mean	KTB02I		0.0383 ± 0.0030
11.5	KGL02	CT	0.0381
14.5	KGL02	CT	0.0396
46	KGL02	CT	0.0354
56	KGL02	CT	0.0349
76	KGL02	CT	0.0394
111	KGL02	CT	0.0359
140	KGL02	CT	0.0412
154	KGL02	CT	0.0412
166	KGL02	CT	0.0366
190	KGL02	CT	0.0357
Mean	KGL02		0.0378 ± 0.0025
2–3	PLDS 79	CT	0.0369
4–5	PLDS 79	CT	0.0360
5–6	PLDS 79	CT	0.0450
8–9	PLDS 79	CT	0.0374
13–14	PLDS 79	CT	0.0395
16–17	PLDS 79	CT	0.0397
19–20	PLDS 79	CT	0.0352
21–22	PLDS 79	CT	0.0386
23–24	PLDS 79	CT	0.0347
26–27	PLDS 79	CT	0.0372
29–30	PLDS 79	CT	0.0330
32–33	PLDS 79	CT	0.0309
34–35	PLDS 79	CT	0.0380
36–37	PLDS 79	CT	0.0396
Mean	PLDS 79		0.0373 ± 0.0034
3–4	TT013-27	CT	0.0367
6–7	TT013-27	CT	0.0392
9–10	TT013-27	CT	0.0353
12–13	TT013-27	CT	0.0316
15–17	TT013-27	CT	0.0332
19–21	TT013-27	CT	0.0327
21–23	TT013-27	CT	0.0383
23–25	TT013-27	CT	0.0349
25–26	TT013-27	CT	0.0331
Mean	TT013-27		0.0350 ± 0.0027

CT: chemical treatment (after Paytan et al., 1993).
LST and SPT: heavy liquid separation (van Beek et al., 2002).

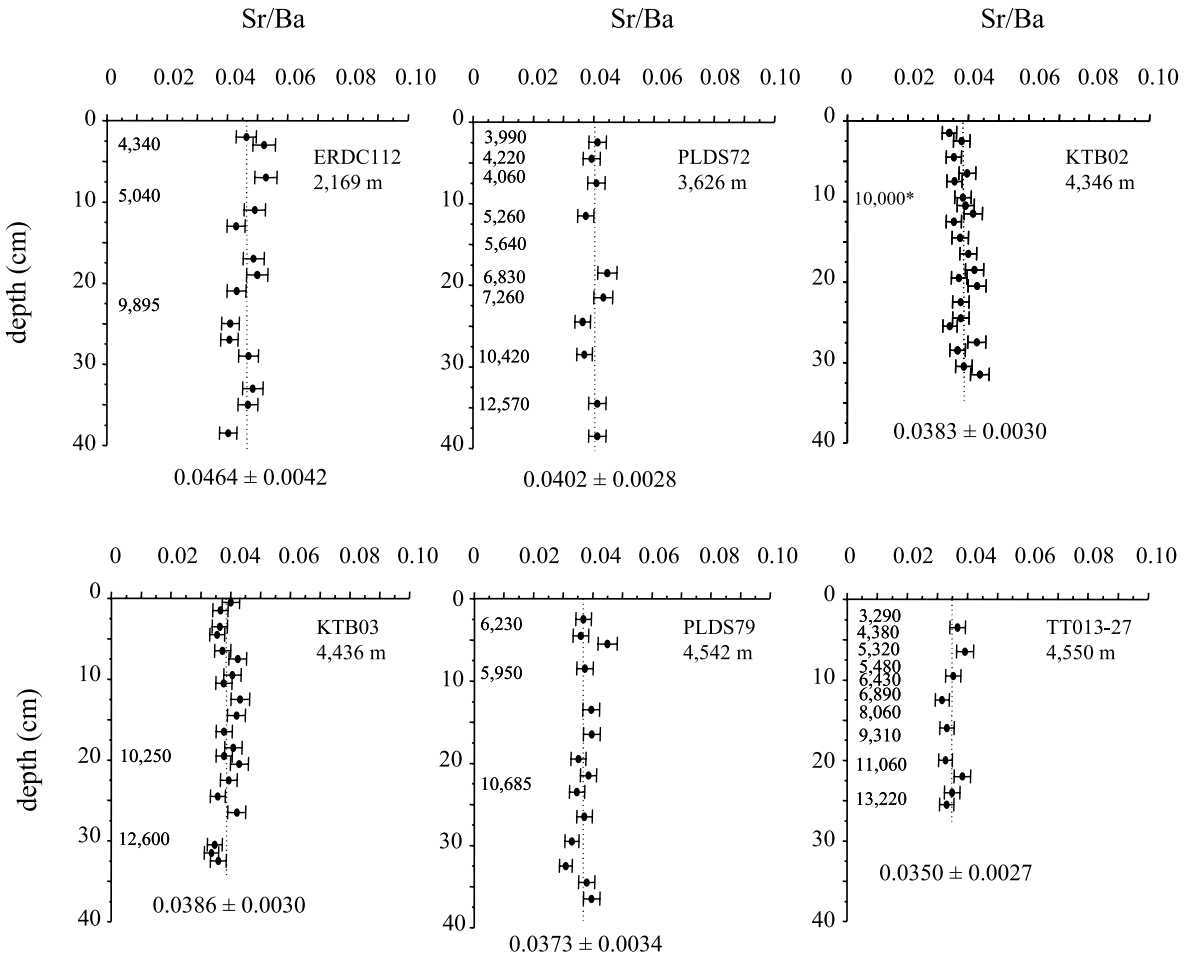

Fig. 3. Profiles of Sr/Ba mole ratios measured in barite samples separated from equatorial Pacific cores. Mean Sr/Ba ratios for each core are shown. Conventional ^{14}C are also reported. * Age estimate based on the sedimentation rate deduced from the ^{226}Ra decay in barite ($\sim$1 cm ka^{-1}; van Beek and Reyss, 2001).

grams of barite as opposed to ratios determined on a single crystal using an electron microscope in previous studies. However, our data appear to fall at the low end of the range found in barite collected in the water column. This result suggests that Sr-rich barite crystals were dissolved preferentially in the water column during settling to the deep-sea floor and/or at the sediment–water interface.

3.2. Sr/Ba ratio: an indicator of barite preservation?

Comparison between the mean Sr/Ba ratios in barite allows us to investigate both water depth and geographic effects on the Sr/Ba ratios. Barium and strontium concentrations in surface waters do not vary significantly in the Pacific (Wolgemuth and Broecker, 1970; Bernat et al., 1972; Chan et al., 1976; Bernstein et al., 1987). One can therefore assume that the Sr/Ba ratio recorded by barite crystals does not vary with longitude in relationship with different hydrological patterns. The same assumptions were made for the ratios from the Atlantic and Indian sectors of the Southern Ocean.

In addition, Monnin et al. (1999) and Rushdi et al. (2000) used thermodynamic models based on

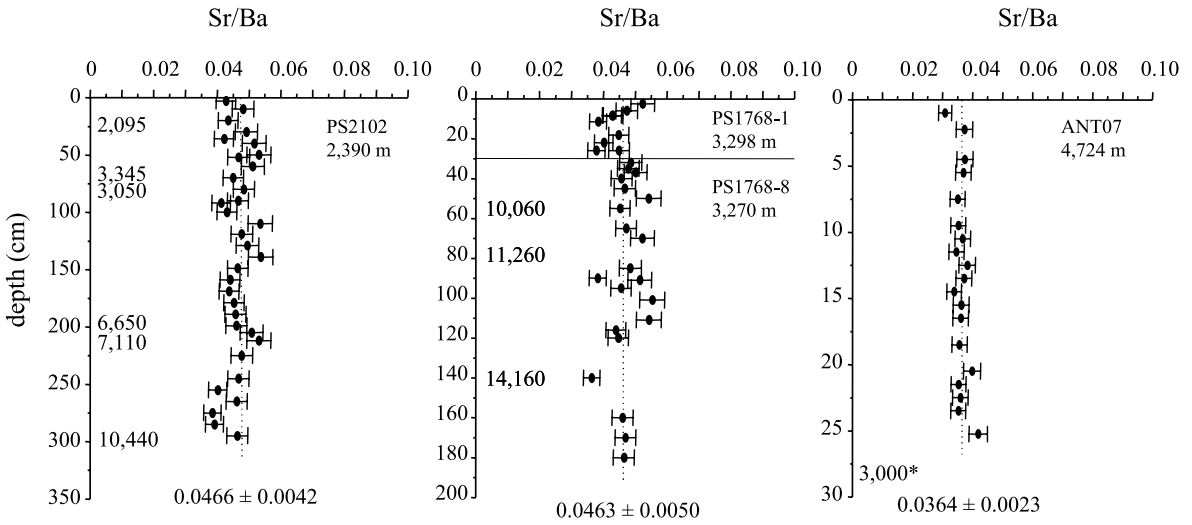

Fig. 4. Profiles of Sr/Ba mole ratios measured in barite samples separated from Southern Ocean cores. Mean Sr/Ba ratios for each core are shown. Conventional ^{14}C ages are also reported. Note the different depth and time scales in between the three cores. Results from multicore PS1768-1 (upper 30 cm) were plotted together with those from the gravity core PS1768-8 considering that 30 cm of the gravity core top was lost during coring operations (Frank, 1996). * Age estimate based on the sedimentation rate deduced from the ^{226}Ra decay in barite (see Fig. 2).

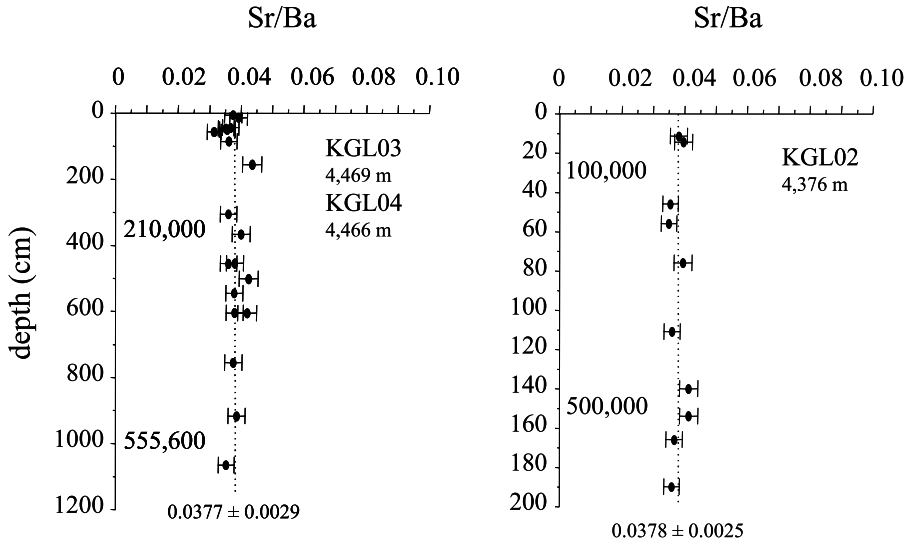

Fig. 5. Profiles of mole Sr/Ba ratios measured in barite samples separated from the gravity cores KGL03-KGL04 (central equatorial Pacific) and KGL02 (western equatorial Pacific). Mean Sr/Ba ratios for each core are shown. Ages deduced from the $^{230}Th_{ex}$ sedimentation rates (KGL03: 1.9 cm ka^{-1}; KGL02: 0.3 cm ka^{-1}; van Beek and Reyss, 2001) are shown in the figure to provide a time reference. Gravity cores KGL03 and KGL04 were collected at the same location as multicore KTB03, whereas gravity core KGL02 was collected at the same location as multicore KTB02. As a comparison, the mean Sr/Ba ratio in barite separated from core KTB03 is 0.0386 ± 0.0030 whereas the ratio from core KTB02 is 0.0383 ± 0.0030. Note the different depth scales in between the two cores.

pure barite and Sr-enriched barite, respectively, to quantify the saturation state of seawater with respect to barite. Surface waters from the Southern Ocean appear to be at equilibrium with barite or slightly supersaturated, as previously shown by Jeandel et al. (1996). At depths between approximately 1500 and 2500 m, waters from the Southern Ocean become undersaturated. On the other hand, thermodynamic calculations suggest that surface waters from the Pacific Ocean are undersaturated. Barite saturation is reached at depths between approximately 1000 and 3500 m, with a return to undersaturation below these depths. For both the Southern Ocean and the Pacific Ocean, the degree of barite saturation below the saturation horizon decreases with increasing water depth.

These results also suggested that waters from the entire Pacific Ocean (from 45°S to 50°N) displayed similar barite saturation states. Consequently, the barite saturation state of the water column from the eastern, central and western equatorial Pacific that are the regions investigated in this study can be considered as identical. Mean Sr/Ba ratios in barite from the equatorial Pacific cores can therefore be plotted together versus water depth (Fig. 6). Similar barite saturation states have also been found in different regions of the Southern Ocean, south of 50°S. We therefore consider that waters from the Indian and the Atlantic sectors of the Southern Ocean have the same barite saturation state. Mean Sr/Ba ratios in barite from Southern Ocean cores can also be plotted together versus water depth (Fig. 6). Note that because waters from the Pacific Ocean and from the Southern Ocean display slightly different saturation states with respect to barite – especially when upper waters are considered – the results obtained in the two oceanic areas are shown separately.

All cores from the equatorial Pacific deeper than 4000 m display comparable Sr/Ba ratios in barite, in agreement with no or little longitudinal effect on the ratio (Fig. 6). Core PLDS72 collected at 3626 m gives an intermediate value between that obtained above 3000 m in core ERDC112 and those below 4000 m. Our data therefore suggest that the Sr/Ba ratios in barite from the equatorial Pacific decrease with increasing water depth. The obtained slope is significantly different from zero at the 99% confidence level. Regarding Southern Ocean cores, the mean Sr/Ba ratios also show a decreasing trend with increasing water depth (Fig. 6). The obtained slope is also significantly different from zero at the 99% confidence level. When the Pacific and Southern Ocean values are compared together, ratios below 4000 m and those above 3500 m are similar. This suggests

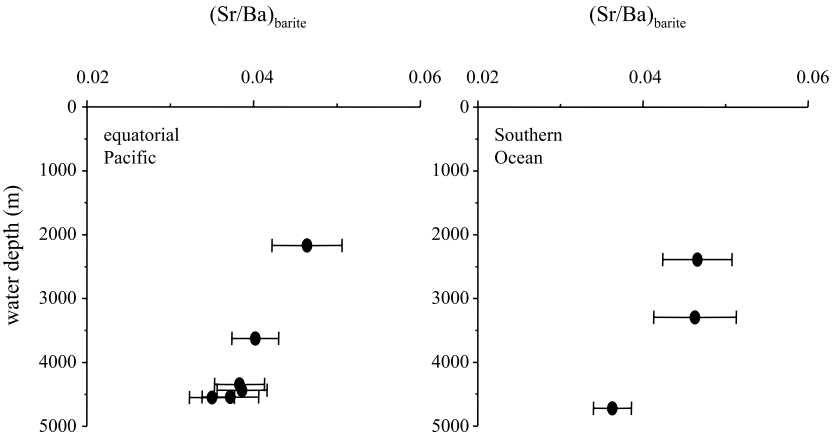

Fig. 6. Mean Sr/Ba mole ratios in barite obtained for each core and reported versus the core water depth, for both the equatorial Pacific and the Southern Ocean. The linear regressions (y being the Sr/Ba ratio and x, the water depth) obtained considering the error bars are for the equatorial Pacific: $y = -4.049 \times 10^{-6}x + 0.055$ ($a = 7.731 \times 10^{-7}$, $b = 0.004$) and for the Southern Ocean: $y = -4.789 \times 10^{-6}x + 0.059$ ($a = 1.204 \times 10^{-6}$, $b = 0.006$), a and b being the standard error of the slope and the standard error of the intercept, respectively.

a comparable geochemical behavior versus water depth within the two oceanic basins. Note that similar ratios obtained in barite separated using two different protocols suggest that the chemical treatment employed does not affect the Sr/Ba ratio in barite, even when strong acids are used. This pattern agrees with the idea that Sr-rich barite crystals dissolve mostly in the water column and/or at the sediment–water interface and are therefore not recovered in deep-sea sediments. If Sr-rich barite crystals were to accumulate in the sediment, one would expect them to be more sensitive to the chemical treatment used in equatorial Pacific sediments (i.e. acids) compared to the one employed in Southern Ocean cores (i.e. heavy liquid).

Sr/Ba ratios of barite from the equatorial Pacific and the Southern Ocean decrease with increasing water depth (Fig. 6). In these two basins, Monnin et al. (1999) and Rushdi et al. (2000) reported a decrease in the degree of barite saturation with increasing water depth below the barite saturation horizon. The decreasing trend in the Sr/Ba ratios may therefore be related to increasing dissolution of barite crystals within undersaturated seawater, with a preferential removal of Sr compared to Ba. This trend is in good agreement with that obtained by Bertram and Cowen (1997), who compared Sr contents of barite crystals from the water column and the deep-sea floor. To some extent, this pattern may be comparable to that observed by McCorkle et al. (1995) when studying elemental ratios (i.e. Cd/Ca, Ba/Ca, Sr/Ca) in benthic foraminifers. These authors gave evidence of a preferential loss of Cd, Ba and Sr during the dissolution of foraminiferal calcite. The original Sr/Ba ratio recorded in barite crystals within the upper water column may therefore be affected during settling to the sea floor and/or at the sediment–water interface.

However, Dymond et al. (1992) suggested that barite preservation might be increased by rapid accumulation rate. Although such a pattern has not always been observed (Kumar et al., 1996), it needs to be considered in this study. Cores investigated in the equatorial Pacific do not show a wide range of sedimentation rates (Table 1). Estimates deduced from the ^{226}Ra decay in barite range from 2.0 cm ka^{-1} for core TT013-27 (4550 m) to 3.3 cm ka^{-1} for core PLDS 79 (4542 m), with core KTB02 (4346 m) displaying a slightly lower sedimentation rate (about 1 cm ka^{-1}). Sr/Ba ratios in barite from cores TT013-27, PLDS79 and KTB02 collected at similar water depths are not significantly different, in spite of the discrepancies observed in the sedimentation rates.

On the other hand, core PS2102-2 displays the highest sedimentation rate of the three cores investigated in the Southern Ocean (31.5 cm ka^{-1}, van Beek et al., 2002). The mean Sr/Ba ratio in barite also appears to be high in this core. Such a pattern may therefore be related to the high sedimentation rate found at this location, which may have led to enhanced barite preservation. However, core PS1768-8, which is characterized by a much lower sedimentation rate (6.4 cm ka^{-1}; Frank, 1996), does not show a mean Sr/Ba ratio significantly different from that of core PS2102-2. Finally, core ANT07 displays a sedimentation rate close to that of core PS1768-8 (9.2 cm ka^{-1}, this study). However, the mean Sr/Ba ratio in barite appears to be lower in core ANT07, a core that was collected deeper in the water column. The higher Sr/Ba ratios in barite are therefore not associated with higher sedimentation rates and vice versa. Sr/Ba ratios rather seem to exhibit a water-depth dependence that may be associated with the dissolution of barite crystals in undersaturated waters (as the undersaturation with respect to barite increases with increasing water depth).

3.3. Sr/Ba ratio of barite in waters at equilibrium with respect to barite

Thermodynamic calculations considering pure barite (Monnin et al., 1999) and Sr-enriched barite (Rushdi et al., 2000) indicated that equilibrium between barite and seawater might be reached in some areas. These results suggested that while intermediate waters of the Pacific and upper waters from the Southern Ocean were at equilibrium with respect to barite, a return to undersaturation occurred below approximately 3000–3500 m in the Pacific and approximately 2000–2500 m in

the Southern Ocean. If these results can be extrapolated to marine barite, one may expect to find such a trend in the Sr/Ba ratio in barite, in case this ratio is a reliable indicator of barite preservation. Barite crystals from cores bathed in waters at equilibrium with respect to barite should indeed not be affected by dissolution. Consequently, constant Sr/Ba ratios in barite are expected to be found at intermediate depths in the Pacific Ocean (between about 1000 and 3500 m) and in the upper 2500 m in the Southern Ocean. Below these depths, the Sr/Ba ratio should decrease with increasing water depth, once barite crystals reach undersaturated waters. However, additional data are needed to confirm or discount such a trend. More cores should obviously be investigated, especially in the upper 3500 m in the Pacific and in the upper 2500 m in the Southern Ocean. It would also be interesting to study other oceanic areas characterized by different barite saturation states [e.g. Bay of Bengal characterized by supersaturated deep waters (Monnin et al., 1999)] so that the behavior of the Sr/Ba ratio in barite can be further tested.

3.4. Paleoceanographic implications

Paleoceanographic investigations often assume that Ba or barite distributions in deep-sea sediments solely reflect a productivity signal while barite preservation is considered constant with time (Schmitz, 1987; Nürnberg et al., 1997; Thompson and Schmitz, 1997). However, acceptance of this pathway is largely the result of the absence of any information regarding the geochemical behavior of barite in the past. Only a few reconstructions take barite dissolution into account. In particular, the relationship proposed by Paytan et al. (1996a) in the equatorial Pacific is based on barite samples separated from core top sediments which allow these authors to incorporate the dissolution effect. Reconstructions performed using the algorithm of Dymond et al. (1992) may also to some extent take barite dissolution into account by including a correction factor that considers the mass accumulation rate and the seawater barium concentrations at the investigated sites. However, such a correction does not take into account the different barite saturation states that characterize each oceanic basin.

The relationship between Sr/Ba ratios in barite and water depth suggests that the Sr/Ba ratio in barite is sensitive to dissolution. The Sr/Ba ratio in sedimentary barite may therefore be useful for the purpose of distinguishing between changes in productivity versus changes in barite preservation when barite distributions are investigated in the sediment. However, as the range of the Sr/Ba ratios in barite between shallow and deep sediments is narrow, one may expect to find only little variation associated with the changes in barite preservation. Slight changes in the Sr/Ba ratios may thus not be easily detected. Investigations conducted with ICP/MS may help reduce the errors on the ratios.

Caution should be nevertheless given when comparisons of barite accumulation rates are to be made for the purpose of paleoproductivity reconstruction between cores collected at different water depths and/or in different oceanic basins. A correction for barite dissolution may indeed be required. Such a correction should depend on the barite saturation state of the water column at the investigated site. Similar conclusions were given by Fagel et al. (2002).

4. Conclusion

Profiles of Sr/Ba ratios in barite separated from sediment cores from the equatorial Pacific and the Southern Ocean display little downcore variation. The Sr/Ba ratios in sedimentary barite appear to fall at the low end of the range found in barite collected in the water column, indicating that Sr-rich barite crystals dissolve preferentially in the water column during settling to the deep-sea floor and/or at the sediment–water interface.

Our results suggest that the Sr/Ba ratios in barite from the Pacific Ocean and the Southern Ocean decrease with increasing water depth. In these two basins, thermodynamic models showed that, over the water depths investigated in this study, the degree of barite saturation in the water column decreased with increasing water depth (Monnin et al., 1999; Rushdi et al., 2000). This

suggests that the dissolution of barite crystals in undersaturated waters may affect the Sr/Ba ratio. This relationship makes the Sr/Ba ratio a potential indicator of the preservation state of barite crystals. However, further investigations obviously need to be conducted (i.e. shallow cores from the equatorial Pacific and the Southern Ocean; cores from other oceanic areas characterized by different barite saturation states) to confirm the pattern observed in this preliminary work. This, in turn, will allow better understanding of the factors that control the preservation of marine barite.

Acknowledgements

We thank Adina Paytan and an anonymous reviewer for their comments that improved significantly the quality of the manuscript. We are grateful to the SCRIPPS Institution of Oceanography, La Jolla, and especially to Warren Smith for providing sediment samples from ERDC and PLDS cores, as well as to the Alfred Wegener Institute, Bremerhaven, and especially to Rainer Gersonde, Michiel Rutgers van der Loeff, Gerhard Kuhn, and Hanes Grobe for providing sediment samples from cores PS2102-2, PS1768-1 and PS1768-8. We thank Dave DeMaster for providing sediment samples from core TT013-27. We are grateful to Olivier Marchal, Roger François and Raja Ganeshram for constructive discussions about the paper. We also thank Charlotte Riccio, Thierry Sampierri and Jean-Louis Saury at the LSM as well as Sophie Ayrault, Serge Boiziau and Denis Piccot at the Laboratoire Pierre Süe, Saclay. We are also grateful to the crew and masters of R.V. *Marion Dufresne* and of R.V. *l'Atalante*. This work was supported by the CEA, CNRS, PROOF 'barytine' (a French CNRS-INSU research program) and partly by a Lavoisier fellowship from the French Ministry of Foreign Affairs.

References

Barnola, J.-M., Raynaud, D., Korotkevich, Y.S., Lorius, C., 1987. Vostok ice core provides 160,000-year record of atmospheric CO_2. Nature 329, 408–413.

Berger, W.H., Killingley, J.S., 1982. Box cores from the equatorial Pacific: ^{14}C sedimentation rates and benthic mixing. Mar. Geol. 45, 93–125.

Berger, W.H., Finkel, R.C., Killingley, J.S., Marchig, V., 1983. Glacial-Holocene transition in deep-sea sediments: manganese-spike in the east-equatorial Pacific. Nature 303, 231–233.

Bernat, M., Church, T., Allegre, C., 1972. Barium and strontium concentrations in Pacific and Mediterranean sea water profiles by direct isotope dilution mass spectrometry. Earth Planet. Sci. Lett. 16, 75–80.

Bernstein, R.E., Betzer, P.R., Feely, R.A., Byrne, R.H., Lamb, M.F., Michaels, A.F., 1987. Acantharian fluxes and strontium to chlorinity ratios in the North Pacific Ocean. Science 237, 1490–1494.

Bernstein, R.E., Byrne, R.H., Betzer, P.R., Greco, A.M., 1992. Morphologies and transformations of celestite in seawater: the role of acantharians in strontium and barium geochemistry. Geochim. Cosmochim. Acta 56, 3273–3279.

Bernstein, R.E., Byrne, R.H., Schijf, J., 1998. Acantharians: a missing link in the oceanic biogeochemistry of barium. Deep-Sea Res. II 45, 491–505.

Bertram, M.A., Cowen, J.P., 1997. Morphological and compositional evidence for biotic precipitation of marine barite. J. Mar. Res. 55, 577–593.

Bishop, J.K.B, 1988. The barite-opal-organic carbon association in oceanic particulate matter. Nature 332, 341–343.

Chan, L.H., Edmond, J.M., Stallard, R.F., Broecker, W.S., Chung, Y.C., Weiss, R.F., Ku, T.L., 1976. Radium and barium at GEOSECS stations in the Atlantic and Pacific. Earth Planet. Sci. Lett. 32, 258–267.

Chow, T.J., Goldberg, E.D., 1960. On the marine geochemistry of barium. Geochim. Cosmochim. Acta 20, 192–198.

Church, T.M., Wolgemuth, K., 1972. Marine barite saturation. Earth Planet. Sci. Lett. 15, 35–44.

Dehairs, F., Chesselet, R., Jedwab, J., 1980. Discrete suspended particles of barite and the barium cycle in the open ocean. Earth Planet. Sci. Lett. 49, 528–550.

Dehairs, F., Goeyens, L., Stroobants, N., Bernard, P., Goyet, C., Poisson, A., Chesselet, R., 1990. On suspended barite and the oxygen minimum in the Southern Ocean. Glob. Biogeochem. Cycles 4, 85–102.

Dehairs, F., Stroobants, N., Goeyens, L., 1991. Suspended barite as tracer of biological activity in the Southern Ocean. Mar. Chem. 35, 399–410.

Dehairs, F., Baeyens, W., Goeyens, L., 1992. Accumulation of suspended barite at mesopelagic depths and export production in the Southern Ocean. Science 258, 1332–1335.

DeMaster, D.J., Pope, R.H., Ragueneau, O., Smith, C.R., 1996. Burial rates of biogenic material along the EqPac transect: Holocene variability and paleoflux indicators. Abstract: Ocean Sciences Meeting, San Diego, CA, p. 42.

Dymond, J., Suess, E., Lyle, M., 1992. Barium in deep-sea sediment: A geochemical proxy for paleoproductivity. Paleoceanography 7, 163–181.

Fagel, N., Dehairs, F., Andre, L., Bareille, G., Monnin, C., 2002. Ba distribution in surface Southern Ocean sediments and export production estimates. Paleoceanography 17, 1–20.

François, R., Honjo, S., Manganini, S.J., Ravizza, G.E., 1995. Biogenic barium fluxes to the deep sea: Implications for paleoproductivity reconstruction. Glob. Biogeochem. Cycles 9, 289–303.

Frank, M., 1996. Reconstitution of late Quaternary environmental conditions applying the natural radionuclides ^{230}Th, ^{10}Be, ^{231}Pa and ^{238}U: a study of deep-sea sediments from the eastern sector of the Antarctic Circumpolar Current System. Ph.D. Thesis. Alfred Wegener Institut, Bremerhaven, Germany.

Gingele, F., Dahmke, A., 1994. Discrete barite particles and barium as tracers of paleoproductivity in South Atlantic sediments. Paleoceanography 9, 151–168.

Guichard, F., Church, T.M., Treuil, M., Jaffrezic, H., 1979. Rare earths in barites: distribution and effects on aqueous partitioning. Geochim. Cosmochim. Acta 43, 983–997.

Jeandel, C., Dupré, B., Lebaron, G., Monnin, C., Minster, J.-F., 1996. Longitudinal distributions of dissolved barium, silica and alkalinity in the western and southern Indian Ocean. Deep-Sea Res. I 43, 1–31.

Kumar, N., Anderson, R.F., Biscaye, P., 1996. Remineralization of particulate authigenic trace metals in the Middle Atlantic Bight: implications for proxies of export production. Geochim. Cosmochim. Acta 60, 3383–3397.

Legeleux, F., Reyss, J.-L., 1996. Ra-228/Ra-226 activity ratio in oceanic settling particles: Implications regarding the use of barium as a proxy for paleoproductivity reconstruction. Deep-Sea Res. I 43, 1857–1863.

McCorkle, D., Martin, P.A., Lea, D.W., Klinkhammer, G.P., 1995. Evidence of a dissolution effect on benthic foraminiferal shell chemistry; δ^{13}C, Cd/Ca, Ba/Ca, and Sr/Ca results from the Ontong Java Plateau. Paleoceanography 10, 699–714.

McManus, J., Berelson, W.M., Hammond, D.E., Klinkhammer, G.P., 1999. Barium cycling in the North Pacific: Implications for the utility of Ba as a paleoproductivity and paleoalkalinity proxy. Paleoceanography 14, 53–61.

Martin, E.E., Macdougall, J.D., Herbert, T.D., Paytan, A., Kastner, M., 1995. Strontium and neodymium isotopic analyses of marine barite separates. Geochim. Cosmochim. Acta 59, 1353–1361.

Monnin, C., Jeandel, C., Cattaldo, T., Dehairs, F., 1999. The marine barite saturation state of the world's oceans. Mar. Chem. 65, 253–261.

Moore, W.S., Dymond, J., 1991. Fluxes of Ra-226 and barium in the Pacific Ocean: The importance of boundary processes. Earth Planet. Sci. Lett. 107, 55–68.

Neftel, A., Oeschger, H., Staffelbach, T., Stauffer, B., 1988. CO_2 record in the Byrd ice core 50,000-5,000 years BP. Nature 331, 609–611.

Nürnberg, C.C., Bohrmann, G., Schlüter, M., 1997. Barium accumulation in the Atlantic sector of the Southern Ocean: Results from 190,000-year records. Paleoceanography 12, 594–603.

Paytan, A., Kastner, M., Martin, E.E., Macdougall, J.D., Herbert, T., 1993. Marine barite as a monitor of seawater strontium isotope composition. Nature 366, 445–449.

Paytan, A., Kastner, M., Chavez, F.P., 1996a. Glacial to Interglacial fluctuations in productivity in the equatorial Pacific as indicated by marine barite. Science 274, 1355–1357.

Paytan, A., Moore, W.S., Kastner, M., 1996b. Sedimentation rate as determined by ^{226}Ra activity in marine barite. Geochim. Cosmochim. Acta 60, 4313–4319.

Paytan, A., Kastner, M., 1996. Benthic Ba fluxes in the central equatorial Pacific, implications for the oceanic Ba cycle. Earth Planet. Sci. Lett. 142, 439–450.

Paytan, A., Kastner, M., Campbell, D., Thiemens, M.H., 1998. Sulfur isotopic composition of cenozoic seawater sulfate. Science 282, 1459–1462.

Reyss, J.-L., Schmidt, S., Legeleux, F., Bonte, P., 1995. Large, low background well-type detectors for measurements of environmental radioactivity. Nucl. Instr. Meth. A 357, 391–397.

Rushdi, A., McManus, J., Collier, R., 2000. Marine barite and celestite saturation in seawater. Mar. Chem. 69, 19–31.

Schmitz, B., 1987. Barium, equatorial high productivity, and the northward wandering of the Indian continent. Paleoceanography 2, 63–77.

Stroobants, N., Dehairs, F., Goeyens, L., Vanderheijden, N., Van Grieken, R., 1991. Barite formation in the Southern Ocean water column. Mar. Chem. 35, 411–421.

Thompson, E.I., Schmitz, B., 1997. Barium and the late Paleocene δC-13 maximum: Evidence of increased marine surface productivity. Paleoceanography 12, 239–254.

van Beek, P., Reyss, J.-L., 2001. ^{226}Ra in marine barite: new constraints on supported ^{226}Ra. Earth Planet. Sci. Lett. 187, 147–161.

van Beek, P., Reyss, J.-L., Gersonde, R., Paterne, M., Rutgers van der Loeff, M., Kuhn, G., 2002. ^{226}Ra in barite: absolute dating of Holocene Southern Ocean sediments and reconstruction of sea-surface reservoir ages. Geology 30, 731–734.

van Beek, P., Reyss, J.-L., DeMaster, D., Paterne, M., in press. ^{226}Ra-in marine barite: Relationship with carbonate dissolution and sediment focusing in the equatorial Pacific. Deep-Sea Res. I.

Wolgemuth, K., Broecker, W.S., 1970. Barium in sea water. Earth Planet. Sci. Lett. 8, 372–378.